The software defined implantable modular platform (STELLA) for preclinical deep brain stimulation research in rodents

IOP Publishing J. Neural Eng. 18 (2021) 056032 https://doi.org/10.1088/1741-2552/ac23e1

Journal of Neural Engineering

OPEN ACCESS

RECEIVED
10 May 2021

REVISED
13 August 2021

ACCEPTED FOR PUBLICATION
6 September 2021

PUBLISHED
21 September 2021

PAPER

The software defined implantable modular platform (STELLA) for preclinical deep brain stimulation research in rodents

Franz Plocksties[1,7,*], Maria Kober[2,7], Christoph Niemann[1], Jakob Heller[1], Mareike Fauser[2], Martin Nüssel[2], Felix Uster[1], Denise Franz[3], Monique Zwar[3], Anika Lüttig[4], Justin Kröger[5], Jörg Harloff[5], Axel Schulz[5], Angelika Richter[4], Rüdiger Köhling[2], Dirk Timmermann[1,8] and Alexander Storch[2,6,8]

[1] Institute of Applied Microelectronics and Computer Engineering, University of Rostock, 18119 Rostock, Germany
[2] Department of Neurology, University of Rostock, 18147 Rostock, Germany
[3] Institute of Physiology, University of Rostock, 18057 Rostock, Germany
[4] Institute of Pharmacology, Pharmacy and Toxicology, University of Leipzig, 04103 Leipzig, Germany
[5] Institute of Chemistry, University of Rostock, 18059 Rostock, Germany
[6] German Center for Neurodegenerative Diseases (DZNE) Rostock/Greifswald, 18147 Rostock, Germany
[7] Contributed equally to this work and share first authorship.
[8] Share senior authorship.
[*] Author to whom any correspondence should be addressed.

E-mail: franz.plocksties@uni-rostock.de

Keywords: deep brain stimulation, low power, long-term, fully implantable, lightweight, DBS stimulator, open source data

Supplementary material for this article is available online

Abstract

Context. Long-term deep brain stimulation (DBS) studies in rodents are of crucial importance for research progress in this field. However, most stimulation devices require jackets or large head-mounted systems which severely affect mobility and general welfare influencing animals' behavior. *Objective.* To develop a preclinical neurostimulation implant system for long-term DBS research in small animal models. *Approach.* We propose a low-cost dual-channel DBS implant called software defined implantable platform (STELLA) with a printed circuit board size of Ø13 × 3.3 mm, weight of 0.6 g and current consumption of 7.6 μA/3.1 V combined with an epoxy resin-based encapsulation method. *Main results.* STELLA delivers charge-balanced and configurable current pulses with widely used commercial electrodes. While *in vitro* studies demonstrate at least 12 weeks of error-free stimulation using a CR1225 battery, our calculations predict a battery lifetime of up to 3 years using a CR2032. Exemplary application for DBS of the subthalamic nucleus in adult rats demonstrates that fully-implanted STELLA neurostimulators are very well-tolerated over 42 days without relevant stress after the early postoperative phase resulting in normal animal behavior. Encapsulation, external control and monitoring of function proved to be feasible. Stimulation with standard parameters elicited c-Fos expression by subthalamic neurons demonstrating biologically active function of STELLA. *Significance.* We developed a fully implantable, scalable and reliable DBS device that meets the urgent need for reverse translational research on DBS in freely moving rodent disease models including sensitive behavioral experiments. We thus add an important technology for animal research according to 'The Principle of Humane Experimental Technique'—replacement, reduction and refinement (3R). All hardware, software and additional materials are available under an open source license.

1. Introduction

As an addition to pharmacotherapy, deep brain stimulation (DBS) is an important therapeutic option in the treatment of movement disorders—particularly for Parkinson's disease (PD), dystonia, and essential tremor [1]. In addition, several novel indications such as epilepsy, Alzheimer's disease, post-stroke recovery and psychiatric disorders are being experimentally explored [2–5]. Although DBS is widely implemented into the clinical routine, its underlying principles and mechanisms are still not fully understood [6, 7].

Indeed, novel questions on long-term benefits, minimizing side-effects such as cognitive dysfunction and optimal targeting for instance regarding dystonia and tremor still need to be addressed [1, 7]. Likewise, bio-markers for therapeutic efficacy are being discussed extensively and need to be confirmed [8]. To investigate these pressing issues, a consequent reverse translational research strategy from bedside back to bench is indispensable. For this purpose, long-term (chronic) DBS instrumentation in freely moving rodents as the best established small animal models for most DBS target diseases is urgently needed [9–12]. The current research field, however, is dominated by severely runtime-restricted implants or back- and head-mounted or wired approaches which do not sufficiently match the requirements for preclinical research. Moreover, animal welfare is significantly impaired by relevant stress to the animals during chronic instrumentation with most current DBS systems used.

For reliable and reproducible long-term DBS experiments in rodents, a DBS system has to meet a sharp requirement profile:

- Stimulation: uninterrupted and constant current stimulation should be delivered for up to 2 months in either unilateral or synchronized bilateral fashion. Since electrodes are complex in production (custom-made electrodes are thus not available at most institutions), stimulation needs to be delivered through commercially available electrodes with the commonly used parameters in chronic DBS research [13–20].
- Implantability: the whole device must be subcutaneously implantable in a single encapsulation including the battery to largely avoid infections and influence on the rodents' social behavior and to allow for preclinical behavioral testing such as Morris Water Maze or MotoRater testing. To achieve this, the stimulator ought to be miniaturized with a maximum weight of 10% of the animal's weight.
- Safety and Reproducibility: charge balanced stimulation is mandatory to avoid adverse electrochemical reactions and subsequent tissue damage. A monitoring system should verify proper stimulation and avoid faulty functioning. This includes control of the reversal pulse caused by the charge balancing method used.
- Expandability: a modular approach for adapting batteries regarding size, weight, and stimulation duration is required, as well as a modular system architecture allowing further extensions like radio and sensory modules. This excludes highly integrated solutions as they are not modifiable or reproducible in an inexpensive and fast manner.

Several groups have developed stimulators for various experimental settings. Table 1 provides all key information of state-of-the-art stimulation devices for preclinical DBS research in rodents. Typical neurostimulators consist of a programmable, miniaturized, battery driven unit to deliver charge balanced stimulation pulses. Reported non-implantable current-driven unilateral or bilateral head or back mountable stimulators have a total weight (including battery with or without housing) of 2.5–16 g applying compliance voltages between 3 and 20 V most often using active or passive charge balancing [21–29]. Subcutaneously implantable neurostimulators weigh 2.5 g (energy supply by induction coil) and 2–13 g (including battery and housing), deliver 2.1 up to 34 V compliance voltages using active or passive charge balancing [30–34]. In both categories, stimulation devices are mostly controlled mechanically by a pushbutton or jumper or wirelessly by a magnet or electromagnetic waves. Sometimes, they provide status readout including information on battery voltage, load impedance and various program variables indicated by a visible or infrared LED or wirelessly by an end device.

As none of the stimulation devices described is able to meet all of the requirements either in terms of volume, weight or battery runtime or functionality or implantability (refer to table 1 and figure 1 for details on volume and battery runtime), we designed and prototyped a new stimulation platform called software defined implantable platform (STELLA), which fulfils all major requirements for the needed reverse translational research approaches.

2. Methodology

Current research efforts in preclinical DBS research are obstructed by limited availability of inexpensive and reliable neurostimulation devices for small laboratory animal models such as rodents. This is particularly the case for detailed open source information on design, fabrication and implantation of such devices (table 1). We publish all technological data under an open source license at [58]. This includes hardware schematic, software and additional materials. STELLA is thus open for reproduction and modifications to a broad scientific community.

2.1. STELLA

To ensure a wide range of possible research applications, the experimental setup of STELLA is based on two exemplary rodent movement disorder models (unilateral PD rat models and the dystonic dt^{sz} mutant hamster model) and defined in an interdisciplinary working process as described in table 2. The general design of STELLA comes as a combination of different modules delivering a ready-to-use stimulation platform with months of *in vitro* and *in vivo*

Table 1. Comparison of existing neurostimulators with STELLA.

	Ewing (2013) [56]	Kouzani (2017) [27]	Kölbl (2016) [26]	Fluri (2017) [24]	Pinnell (2018) [29]	Adams (2019) [21]	Harnack (2008) [32]	Fleischer (2020) [57]
Current amplitude (μA)	13–1000	200	26–2036	10–500	20–2000	−375–250	50–600	up to 300
Pulse-width (μs)	1 μs-100% DC‡	90	0.5 μs-100% DC‡	60–500	10 μs-100% DC‡	20 (min)	52	60–500
Frequency (Hz)	2–500	130	10–300	10–200	0.1–5000	5000 (max)	131	10–500
Inter-pulse delay (μs)	n/a	n/a	60	n/a	0-pulse period	n/a	n/a	n/a
Compliance voltage (V)	20	3 (battery)	17	3.1 (battery)	12	10	18	3.1 (battery)
No. of channels	2	1	1	1	2	1	1	1
Charge balancing	Passive	Passive	Active	Passive	Active/Passive	Active	Active	Passive
Lifetime (DBS-on)	10 days	22 days	6 days	30 days	30 h	9 h	28 days	30 days
Type of battery	ICP521630PM	CR2032	3xp675	2xV364	CR1225	CR2032	2xSR48	2xV364
Battery weight (g)	5.4	3	3 × 1.8	2 × 0.3	0.9	3	2 × 1.1	2 × 0.3
PCB weight (g)	n/a	0.92	n/a	n/a	0.8	2.18	n/a	n/a
Total stimulator weight (g)	11.5¶	4.75§	13.8¶	2.5§	2.8¶	5§	13¶	2.8§
Battery volume (mm^3)	3052	1000	3 × 550	2 × 70	300	1000	2 × 260	2 × 70
PCB size (mm)	n/a	15 × 18 × 3*	26 × 12 × 3*	n/a	Ø12.5 × 5	30 × 25 × 3*	35 × 17.1 × 3*	10 × 10 × 1
PCB volume (mm^3)	2228	810	936	1477	613	2250	1796	100
PCB + battery volume (mm^3)	5280	1810	2586	1617	913	3250	2316	240
Total stimulator size (mm)	33 × 20 × 8¶	15 × 18 × 10*§	30 × 20 × 24*¶	21 × 11 × 7§	Ø19.2 × 12.4¶	32.5 × 28 × 8§	38.5 × 20 × 13.5¶	n/a
Control medium	Magnet	Pushbutton	n/a	Jumper	Magnet	Magnet	Electromagn.	Magnet
Output medium	Visual LED	Visual LED	n/a	Visual LED	Visual LED	Visual LED	Electromagn.	Visual LED
Status readout	♣	Programming status	n/a	On/Off/♠	On/Off	On/Off/♣	Program var.	On/Off
Mounting	Head or Back	Back	Head	Head	Head	Back	Implant	Implant
Open source†	No	No	No	No	Complete	No	No	No

(Continued.)

Table 1. (Continued.)

	de Haas (2012) [31]	Hentall (2013) [33]	Millard (2007) [34]	Forni (2012) [25]	Alpaugh (2019) [30]	Liu (2017) [28]	Arfin (2009) [22]	STELLA
Current amplitude (μA)	20–100	20–100	100–500	50–120	149	200–500	10–1000	42–100
Pulse-width (μs)	60	100–1000	25–250	0–80	103/111	30–1400	180	1 μs-100% DC[‡]
Frequency (Hz)	131	8, 16 or 24	50–5000	0–130	130	1–200	1400 (max)	10–5000
Inter-pulse delay (μs)	200	n/a	n/a	n/a	103	n/a	n/a	n/a
Compliance voltage (V)	4.65 (battery)	34	5	6 (battery)	2.1	3 (battery)	5	2.2–2.8
No. of channels	2	1	1	1	1	1	4	2
Charge balancing	Active	Passive	Active	n/a	Active	Passive	Active	Passive
Lifetime (DBS-on)	10 h	n/a (rests)	∞	7	30 days	3 months	12 days	126 days (CR1216), 241 days (CR1225) [¤]
Type of battery	3xSR416	2xSR41	None, energy provided through inductive cage	2xCR1220	2xSR48	CR2032	2xML614	CR1216, CR1220, CR1225, CR2032[□]
Battery weight (g)	3 × 0.13	2 × 0.6	—	2 × 0.8	2 × 1.1	3	2 × 0.16	0.6 (CR1216), 0.9 (CR1225) [□]
PCB weight (g)	n/a	n/a	n/a	n/a	n/a	n/a	n/a	0.6
Total stimulator weight (g)	2.1[¶]	2[¶]	2.5[{]	5.6[{]/7.4[¶]	4.7[¶]	6[§]/16[¶]	1.3[§]	2.6 (CR1216), 4 (CR1225)[¶ □]
Battery volume (mm^3)	3 × 30	2 × 160	—	2 × 250	2 × 260	1000	2 × 50	200 (CR1216), 300 (CR1225) [□]
PCB size (mm)	25 × 8 × 3[*]	n/a	n/a	28 × 9 × 3[*]	n/a	Ø20 × 4	13 × 13 × 3[*]	Ø13 × 3.3
PCB volume (mm^3)	600	688	n/a	756	n/a	1256	507	438
PCB + battery volume (mm^3)	690	1008	—	1256	n/a	2256	607	638 (CR1216), 738 (CR1225) [□]
Total stimulator size (mm)	Ø8 × 30[¶]	18 × 8 × 7[¶]	14 × 12 × 6[{]	15 × 28 × 7[¶]	n/a	Ø20 × 8[¶]	n/a	Ø15.5 × 7.5 (CR1216), Ø17.0 × 9.0 (CR1225)[¶ □]

(Continued.)

Table 1. (Continued.)

	de Haas (2012) [31]	Hentall (2013) [33]	Millard (2007) [34]	Forni (2012) [25]	Alpaugh (2019) [30]	Liu (2017) [28]	Arfin (2009) [22]	STELLA
Control medium	Magnet	Magnet	Electromagn.	n/a	n/a	Electromagn.	Electromagn.	Magnet♦
Output medium	IR LED	IR LED	Visual LED	n/a	Visual LED	Electromagn.	Visual LED	Visual LED♦
Status readout	On/Off/♠	Program var.	On/Off	n/a	♣	On/Off/♣♠	On/Off	On/Off/♣♠♦
Mounting	Head + Implant	Implant	Implant + cage	Head	Implant	Head	Head	Implant
Open source†	No	No	Incomplete	No	No	No	Incomplete	Complete

*Estimated from photographic scale

‡Duty Cycle

Including § battery, { housing, ¶ both

†Including all design/layout/firmware files and datasets for reproduction

¤Refers to the stimulation parameters (1 × 100 μA, 130 Hz, 60 μs) for LPM3 at a boost voltage of 3.1 V

□Highly flexible regarding needed stimulation time and rodent's size and weight

♣Battery voltage/♠load impedance out of range indication

♦Extendable by inter-module communication.

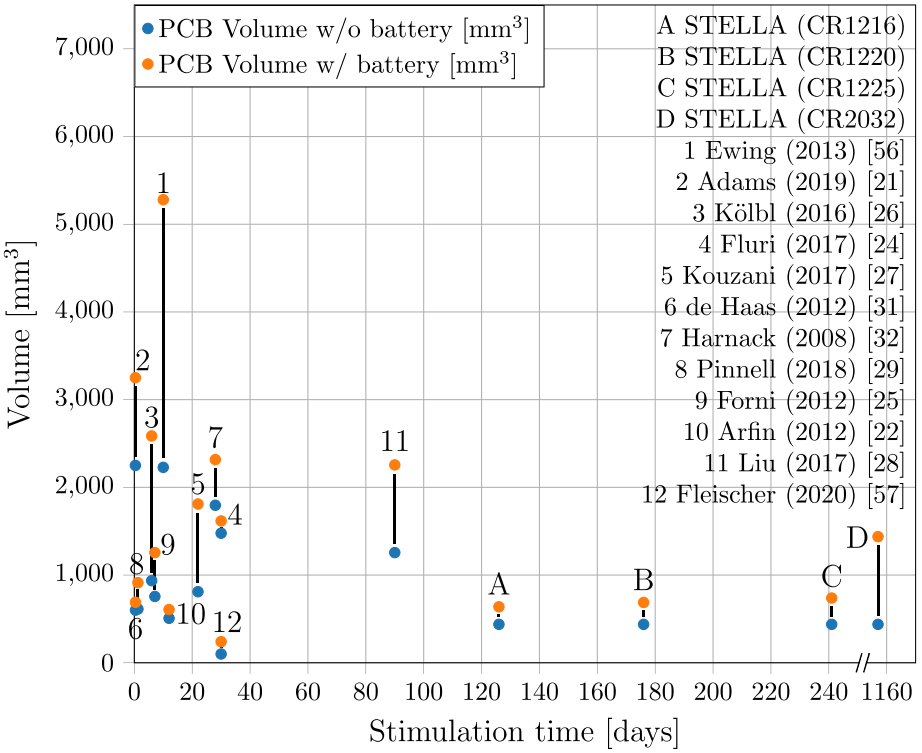

Figure 1. Comparison of volume and stimulation time of current neurostimulators. STELLA's current consumption refers to the stimulation parameters (1 × 100μA, 130 Hz, 60 μs) for LPM3 at a boost voltage of 3.1 V. Battery specifications: RENATA CR1216 (25 mAh), RENATA CR1220 (35 mAh), RENATA CR1225 (48 mAh), VARTA CR2032 (230 mAh).

testing experience applied for design optimization. STELLA consists of:

- Stimulation printed circuit board (PCB): The stimulator was fabricated on a double-sided, four-layer circular PCB with 13 mm diameter and 3.3 mm height yielding a volume of 438 mm^3 and a weight of 0.6 g. It provides a dual channel output that allows for unilateral and bilateral operation at an average power consumption of about 24 μW for DBS (figure 2).
- Software: STELLA comes with a lightweight firmware which utilizes low power modes (LPMs) for optimized battery usage, enabling ultra-long stimulation experiments of 8 months on a CR1225 and 3 years on a CR2032 battery (figure 1).
- Encapsulation scheme: we developed an easily reproducible and inexpensive encapsulation made from medical grade chemicals with high biological compatibility based on the experience of Chang *et al* [35]. The detailed procedure is reported in the supplementary construction manual (available online at stacks.iop.org/JNE/18/056032/mmedia).
- Electrode setup: the ability of a stimulator to constantly deliver the desired current pulse must be ensured. Choosing the right electrode is crucial for a successful DBS setup. The electrode diameter needs to be adapted for the size of rodent brains. The design of the electrode tip determines the electric field distribution and impacts the volume of activated tissue. STELLA's ability to drive the stimulation current was validated with two different electrode setups (table 2). For bipolar stimulation, we opted for the commonly used PI-SNEX-100 (Microprobes, Gaithersburg, USA) that we examined *in vitro* and *ex vivo*. For unipolar stimulation, we designed a customized electrode (manufactured from Microprobes, Gaithersburg, USA) based on previous evidence [20, 36, 37] (supplementary figure S1). The unipolar setup was validated *in vitro, ex vivo* and in a long-term *in vivo* study over 6 weeks.

2.2. Technical realization of stimulation device

The proposed stimulator is loosely based on the device published by Ewing *et al* as starting point for our design [23]. However, almost every part was either changed or enhanced to meet the outlined demands for ultra-long reliable stimulation experiments. The stimulation platform provides a control unit, a power unit, a stimulation and monitoring unit. The control unit is designed around the off-the-shelf MSP430G2553 TI 16 bit microcontroller. It controls stimulation and other functions concerning the device operation by six 8 bit 100 kΩ digital potentiometers. Two of them are combined in one package (AD5142) and the remaining four are combined in another package (AD5144). These digital potentiometers are controlled by the serial peripheral

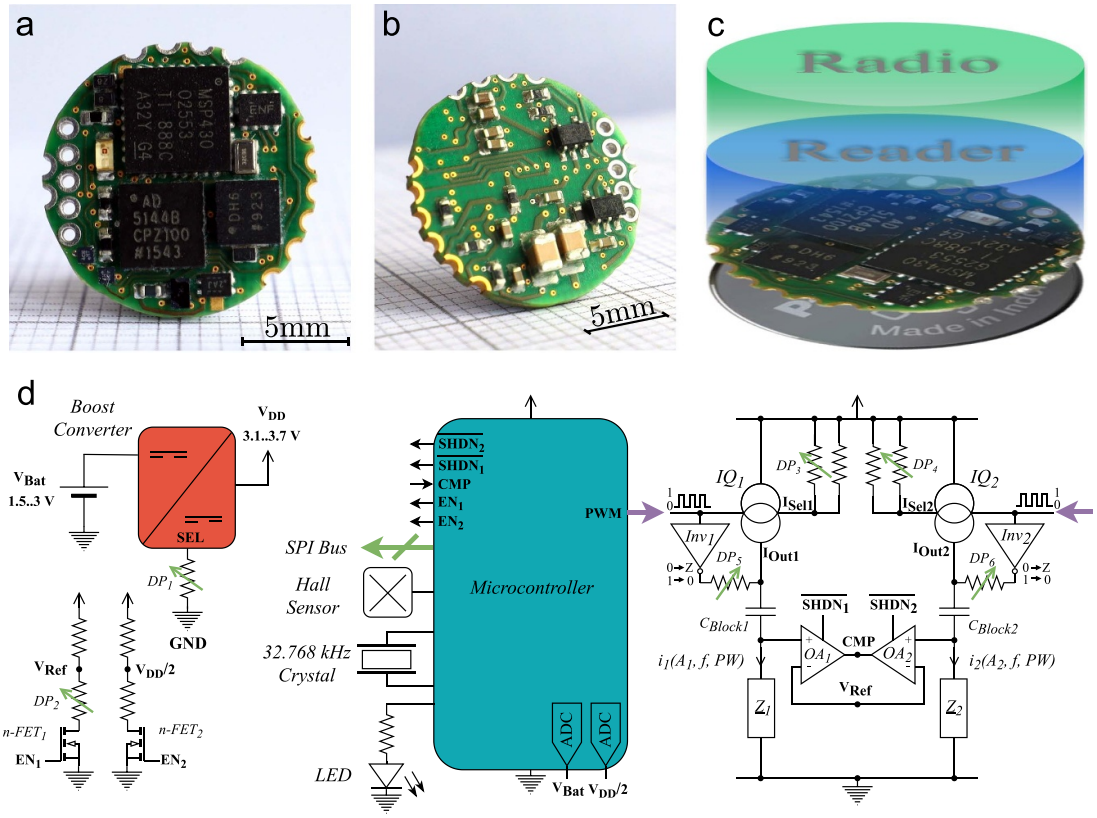

Figure 2. Overall schematic diagram of STELLA. Top (a) and bottom (b) view of the circular STELLA PCB shown on millimeter paper. (a) The left ports provide the programming interface and supply voltage connections. The ports on top provide the stimulation outputs. The ports on the right side serve for inter-module communication. (b) Bottom side. (c) Modular architecture for further possible extensions like sensory and radio module. (d) The Boost Converter steps up the battery voltage V_{Bat} into an overall supply voltage V_{DD}. The Microcontroller activates two current sources IQ_1 and IQ_2 which serve to deliver stimulation pulses to the respective impedances $\underline{Z}_1$ and $\underline{Z}_2$ by a PWM signal sourced by an external 32.768 kHz crystal. It uses the SPI Bus to control six digital potentiometers DP for adapting stimulation parameters (compliance voltage, current amplitudes, discharge resistances) and V_{Ref}. Two inverters Inv_1 and Inv_2 balance the charge passively by grounding the electrodes with an adjustable resistance in that path. The blocking capacitors C_{Block1} and C_{Block2} serve as barrier against a prolonged DC current. The monitoring method activated by a Hall Sensor composed of two operational amplifiers OA_1 and OA_2 and an adjustable reference voltage V_{Ref} detects short and open circuits. The results are indicated by a blink pattern of a LED. The voltages V_{DD} and V_{Bat} are converted by ADC's in digital numbers. The n-channel MOSFET's n-FET_1 and n-FET_2 prevent a permanent current draw through the voltage divider circuits.

interface (SPI) bus supported by the MSP430. The serialized JTAG protocol Spy-Bi-Wire permits flashing and accessing internal registers for on-chip emulation. The stimulation unit, controlled by four digital potentiometers, comprises two current sources (PSSI2021SAY), two blocking capacitors and two inverters with open-drain output (SN74AUP1G06). In addition, we equipped STELLA with a monitoring unit including two operational amplifiers (TLV9002S) in one package and two digital potentiometers. This monitoring feature is remotely activated by a Hall effect sensor (DRV5032AJ). Finally, the power unit includes a 1.5 V or 3 V coin cell and a boost converter (MAX17220). The entire schematic of the proposed circuitry is shown in figure 2(d). The individual parts will be explained below. A detailed description can be found in the supplementary technical manual.

2.2.1. Modularity of batteries and system architectures
The aim of the stimulation system is to have as low interference with the rodents' social behavior as possible. This includes free movement in various environments such as the Morris Water Maze pool. Any external devices such as energy supply or the placement of inductive coils are precluded, particularly since they usually only work at short range or in restricted areas [34]. Therefore, the stimulation device is powered by coin cells as energy source due to their lightweight and circular flat shape that matches our stimulator (see figures 2(a) and (b)). The shape is especially advantageous, since placing the coin cells on top of the stimulator saves tremendous space for one single housing. A boost converter steps up the time-varying input voltage of the battery into a stable supply voltage of 3.1 V for overall system supply. As the booster is able to convert input voltages from 400 mV, typical coin cells yielding a voltage of 1.5 or 3 V can be used. The stabilization of the supply voltage additionally covers battery's voltage drops caused by brief current peaks from the LED or a possible RF module. STELLA offers a high flexibility in the choice of battery capacity due to its low current consumption.

Table 2. Stimulation requirements for DBS studies in rodent movement disorder models[a].

Setting	(1) EPN-DBS or STN-DBS in unilateral Parkinsonian rats	(2) EPN-DBS in dystonic *dt*^{sz} hamster
Pulse-shape	Rectangular	Rectangular
Pulse-width [μs]	60	60
Frequency [Hz]	130	130
Amplitude [μA]	50–100 (unilateral)	100 (unilateral) or 2 × 50 (bilateral)
Channel	Unilateral	Unilateral or bilateral
Stimulation Duration	up to 2 months	3 h to 11 days
Electrode	Unipolar electrode from Microprobes Inc., custom-made, Plastics One Inc.	Bipolar electrode PI-SNEX-100 from Microprobes Inc., custom-made

[a] Stimulation parameters for DBS of entopeduncular nucleus (EPN) or subthalamic nucleus (STN) in various rodent disease models as extracted from the literature [13–20].

This modularity allows adapting the coin cell's weight and size regarding the type of rodent and stimulation setting without affecting their comfort, mobility, and general well-being. This offers a suitable trade-off between size and stimulation time for the specific experiments in animal models of dystonia and PD. STELLA uses SPI to control and adapt intra-module stimulation parameters such as current amplitudes by digital potentiometers which are adjusted by software. In addition, the same bus also serves for inter-module communication to address potential extensions like a radio module and sensory readouts, achieving a stackable and therefore modular system architecture while remaining lightweight and energy efficient in a tiny form factor (see figure 2(c)). Therefore, we routed the pins of the SPI bus to the edge of the PCB making it accessible from outside.

2.2.2. Electrode-tissue impedance and compliance voltage

We conducted extensive *ex vivo* and *in vivo* experiments to assess the needed compliance voltage of the specific setups so the stimulation pulse is not distorted even for varying impedances of the electrodes themselves and of the tissue response to injury caused by electrode implantation [38]. For DBS, we evaluated voltage and current measurements of electrodes in rodents, such as rats and hamsters. In all long-term stimulation setups (see table 2) we found that the voltage of the current source within the DBS pulse generator to supply the current specified, was below 2.8 V inside brain tissue. Typically, it was below 2 V. We opted for a booster approach delivering variable voltages in steps of 100 mV between 3.1 V and 3.7 V for supplying the current source. Due to a drop of the output voltage by 900 mV inside the current source we are able to deliver compliance voltages between 2.2 and 2.8 V at the electrodes. This allows to use a unified voltage approach for electronics and stimulation contributing significantly to ultra-low power operation and a small footprint. STELLA's monitoring system, incorporated into built-in self-test (BIST) discussed later, detects any risk of out of compliance issue and compensates it by controlling a digital potentiometer that adjusts its output voltage automatically. In contrast, other approaches [21, 23, 26, 29, 32, 33] suffer from high compliance voltages affecting the power consumption or area drastically.

2.2.3. Generation of stimulation signal

Mainly, the microcontroller generates a pulse-width-modulation (PWM) signal which allows the precise control of the repetition rate and pulse width of the stimulation signal. This PWM signal drives two current sources. Thereby, synchronized pulses in bilateral operation are guaranteed. If unilateral operation is used, one stimulation output can be left open. Moreover, the PWM signal simultaneously drives the input of two inverters with open drain which control the charge balancing method described in section 2.2.4. For our stimulation requirements (see table 2), we tailored the highly non-linear current source's output regarding a high resolution between 42 and 100 μA to attain high accuracy in this range. This is achieved by an additional 30 kΩ resistance in parallel to each potentiometer's resistance compensating failure tolerances in this range. Here, we achieve a maximum error of 1% for 100 μA and 0.1% for 50 μA. If other requirements for current amplitude and its accuracy are needed, the parallel resistors can easily be replaced (see repository for detailed calculations). Note, the voltage amplitude must not exceed the compliance voltage at any time to ensure that the desired output current is supplied.

2.2.4. Charge-balancing

Even though stimulation patterns differ, the most important criterion for charge balancing is the prevention of tissue damage. While it has been shown that monophasic pulses cause significant harm to tissue, biphasic stimulation pulses do not show this issue [39, 40]. Mainly, in a biphasic stimulation, the desired physiological effect is achieved by the first stimulation pulse, for instance, initiating an action potential [41]. The subsequent reversal pulse is used for compensating the residual charges, as any charge residual left

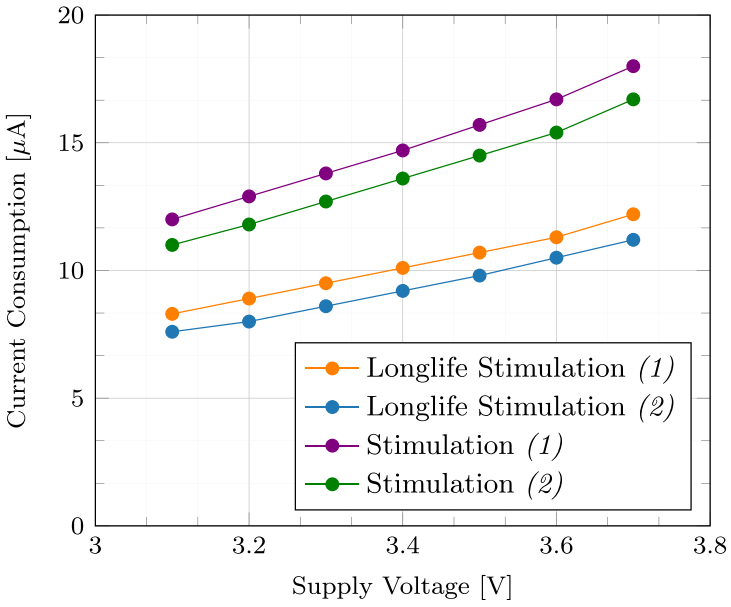

Figure 3. STELLA's current consumption during stimulation by increasing the boost voltage in steps of 100 mV. All measurements were performed for setting (1) at 1 × 100 μA, 60 μs, 130 Hz and for setting (2) at 2 × 50 μA, 60 μs, 130 Hz with 30.5 μs pulse-width resolution (longlife stimulation) and 1 μs pulse-width resolution (stimulation).

will accumulate on the electrode-tissue double layer and harm the tissue due to strong faradaic currents. Consequently, it must be ensured that the net charge for a large number of stimulation periods is zero:

$$Q = \int_{t=0}^{nT} i(t)\,\mathrm{d}t = 0$$

where Q is the net charge, $i(t)$ is the AC current, T is the period and n is the number of periods.

To avoid these adverse electrochemical reactions, we based our design on the established, passive charge balancing scheme by shortening the electrodes to ground after each stimulation cycle [23, 24]. This method leads to a high reversal pulse that might counteract the desired effect of the first stimulation pulse by rapidly hyperpolarizing the cells [41]. To ensure an adequate level of control of this therapeutic effect, we included a resistor in that discharge path for each channel which is adjustable by digital potentiometers that help to flatten this reversal pulse. Note that the discharge period depends on the amount of injected charge, electrode-tissue impedance, and the resistance in above mentioned discharge path. As a safety feature, we therefore placed a DC blocking capacitor in series with each stimulation electrode acting as a barrier to prevent any DC current even if the accumulated charge is not fully discharged in between the stimulation pulses [42]. We have chosen a capacitance of 4.7 μF for the DC blocking capacitor in order not to affect the compliance voltage due to a voltage drop across the capacitor during current integration. This is sufficiently high regarding the stimulation setups outlined in table 2.

2.2.5. Timer and power-saving features

Each component has been carefully selected for minimum power and available LPMs of the controller have been fully exploited and extended as detailed below. The microcontroller executes the main program at 1 MHz in active mode only, however, at the price of highest current consumption. For most of the time, the MCU is in LPM with peripheral and internal clocks shutdown. An external 32.768 kHz crystal clocks a 16 bit timer to generate a PWM signal driving STELLA's stimulation unit. This longlife approach achieves a pulse-width resolution of 30.5 μs by drawing only 8.3 μA/3.1 V (setting (1) in table 2) or 7.6 μA/3.1 (setting (2) in table 2). We also support 1 μs resolution with slightly increased current consumption of only 12 μA/3.1 V (setting (1) in table 2) or 11 μA/3.1 V (setting (2) in table 2). For storage purpose, STELLA can additionally be placed into deep sleep mode by drawing only 4.5 μA/3.1 V.

All current consumption measurements were performed by placing a current waveform analyzer (CX3300A, Keysight) in series with a power supply at 3 V and STELLA. The data were digitized at a sampling frequency of 500 kHz, recorded for a period of 20 s and finally averaged. STELLA's overall current consumption during stimulation over its entire boost voltage range is depicted in figure 3.

2.2.6. Features for reliability and quality of results

The scientific value of an experiment is highly dependent on reproducibility and the exact implementation of its specifications. Therefore, reliability and precision of the equipment are crucial. Furthermore, lab equipment is often custom-made and quality can thus vary. For example, as one factor, we

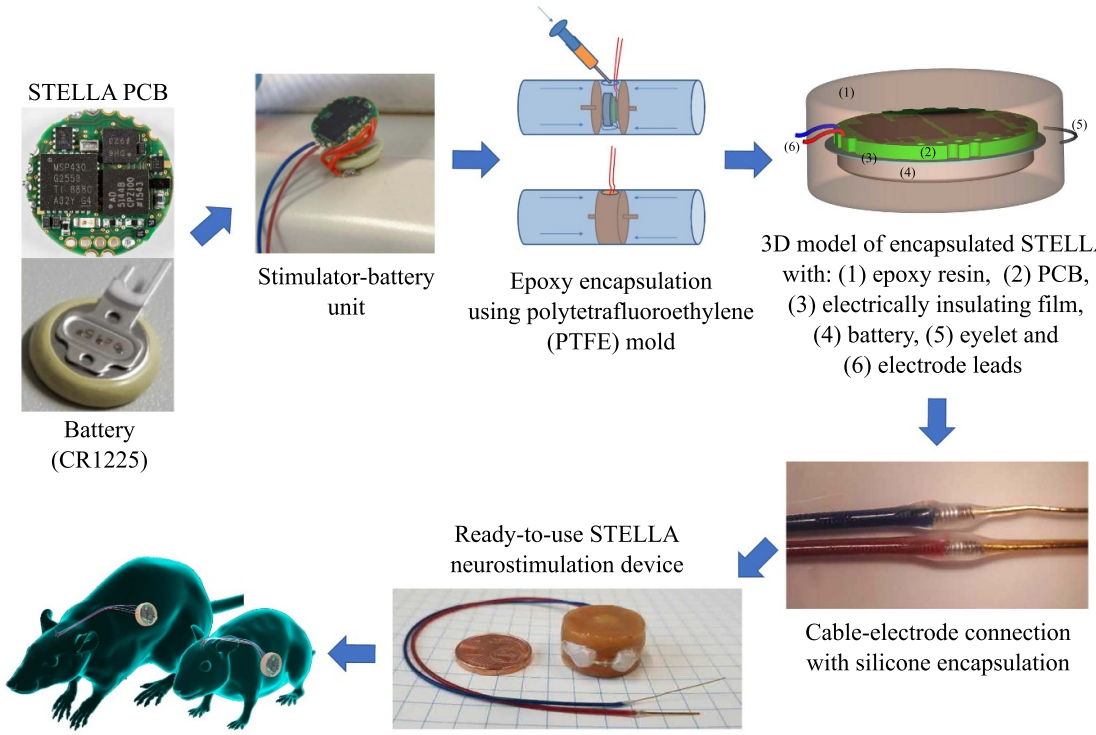

Figure 4. Schematic representation of fabrication, encapsulation and implantation of the STELLA neurostimulation device. Implanted systems for bilateral use in rat and hamster are depicted in true to scale. For details, please refer to the supplemental text material.

found implanted electrodes to vary in their properties; even electrical short and open circuits did occur, either due to an intrinsic defect or due to injury of the electrode during the implantation process. Due to the lack of appropriate tests, such problems typically remain undetected. We implemented a BIST mechanism to automatically detect and report such problems by monitoring the stimulation voltage. A tiny Hall effect sensor initiates this BIST procedure.

2.2.7. Microcontroller Software

STELLA's firmware yielding a size of 5.6 kB was developed in C language within the free integrated development environment (IDE) Code Composer Studio from TI. Using this IDE, the firmware is uploaded into its MSP430's flash memory by accessing the Spy-Bi-Wire PCB pin-out with a TI development board MSP-EXP430G2. Since the MSP430G2553 flash memory provides a size of 16 kB, there is enough space left for further inter-module algorithms. After applying power, the MSP430 processes all user defined values including unilateral/bilateral operation, frequency, pulse-width and pulse-width resolution, current amplitude and discharge resistance. When holding a magnet close to the implant, the Hall sensor is triggered and STELLA's BIST is enabled. This BIST checks whether battery voltage and load impedance are within an appropriate range and if necessary adapts the boost voltage. When this procedure is finished, a LED flashes in a specific pattern such that common failures (low battery voltage, short and open circuits) or a correct function for both channels (bilateral operation) or one channel (unilateral operation) can be detected visually. Furthermore, the Hall sensor can be used to switch stimulation on and off.

2.3. Encapsulation of STELLA DBS device

2.3.1. Encapsulation

We opted for a medical grade epoxy resin encapsulation procedure by using a polytetrafluoroethylene (PTFE, Teflon) mold producing an implant with an extraordinary profile of inexpensive, biocompatible, reproducible and mechanically stable properties (figure 4, see supplementary construction manual for all details). The implant's side includes a small eyelet which allows adequate fixation to the subcutaneous tissue. In brief, wires for the stimulation electrodes (helical stainless steel wires with silicon isolations, 0.7 mm thin lead; Open Source Instruments Inc., Watertown, MA, USA) and wires for energy supply were soldered to the PCB and connected to the battery. We then placed the battery on the ground of the PTFE mold, followed by an electrically insulating PTFE film and the PCB. Subsequently, we filled the PTFE mold with biocompatible epoxy resin (Polytec EP 655 T; Karlsbad, Germany) in a two-step procedure. After the resin has cured for 5.5 h at 62 °C, the

device was smoothened and an eyelet was attached. Finally, the stimulation electrodes were soldered to the thin leads and isolated by two thin layers of silicone (Nusil MED 10-6607; Avantor, Center Valley, PA, USA).

For PCB and self-made encapsulation, the costs for one STELLA implant can be estimated to ∼120€. Prices for electrodes and wires depend on stimulation settings. Explanted stimulators (inclusive wires) are reusable multiple times depending on stimulation period and storage time (see supplementary construction manual). Only electrodes need to be replaced.

2.3.2. Leakage testing

To test the fully encapsulated STELLA implant for corrosion and leakage, we exposed the implant to Neurobasal Plus medium (Gibco, Tulsa, OK, USA), adding 30 mM H_2O_2 at 37 °C for 12 weeks. The implant was fixed to its wires, completely immersed in the medium and mechanically stressed by a stirrer (300 rpm) simulating *in vivo* conditions [43].

The implant was programmed to setting (1) in table 2 (100 μA, 60 μs, 130 Hz) and checked daily by triggering the BIST function with a magnet from outside the solution.

2.4. *In vitro* and *ex vivo* testing of STELLA DBS device

We checked the functionality of STELLA with two different electrode types in brain tissue *ex vivo* and in saline solution *in vitro*. For this purpose, we immersed bipolar (PI-SNEX-100, Microprobes, Gaithersburg, US) and unipolar electrodes (custom-made, Microprobes, Gaithersburg, US) into rat brain tissue *ex vivo* and into 0.9% saline solution *in vitro* by injecting stimulation pulses from STELLA according to table 2. Voltage and current recordings of the stimulation pulses were performed with an oscilloscope. First, the stimulation voltage across the load impedance $\underline{Z}$ (brain tissue or saline solution) was recorded. Afterwards, we placed a shunt resistor R_{Shunt} (329 Ω) to the ground side and measured the voltage across it. Applying Ohm's Law, we were able to calculate the stimulation current. The experimental setup with a bipolar electrode (PI-SNEX-100) and gassing is shown in supplementary figure S2(a) and the measurement setup is presented in supplementary figure S2(b).

Brain slices were derived by transverse cutting using a vibratome (Campden Instruments, Loughborough, United Kingdom) and transferred into a holding chamber containing artificial cerebrospinal fluid gassed with 95% O_2 and 5% CO_2 to maintain the pH at 7.4) essentially as described previously [44–46]. All procedures were performed in accordance with European guidelines (2010/63/EU).

2.5. Preclinical testing of STELLA DBS device

2.5.1. Animal studies

For all animal studies, male adult wild-type Wistar-Han rats (Charles River Laboratories, Sulzfeld, Germany) with a body weight of 300 g were used (∼12 weeks of age). All rats were housed under controlled conditions (12 h dark and light cycle, food and water ad libitum) in a group of two per cage and separated after electrode implantation. All animal experiments were conducted in accordance with European guidelines (2010/63/EU) and permitted by the local animal care committee (Landesamt für Landwirtschaft, Lebensmittelsicherheit und Fischerei, Mecklenburg-Vorpommern, Germany; LALLF M-V/7221.3-1.1-051/17; LALLF M-V/7221.3-1.1-075/18).

2.5.2. Surgery

The stimulation electrode (unipolar platinum electrode, supplementary figure S1) was implanted stereotactically into the right subthalamic nucleus (STN) at the following coordinates relative to bregma [47]: AP −3.8 mm; ML ±2.4 mm, and DV −7.6 mm. A single ground electrode (2 cm gold wire, Ø 250 μm) was implanted subcutaneously outside of the skull dorsal to stimulation electrodes near midline and fixed together with the stimulation electrode with dental cement. 6-Hydroxydopamine (6-OHDA) Hemi-Parkinson induction was performed as reported previously [14]. 6-OHDA sham rats were injected with a solution of 0.02% ascorbic acid and 0.9% sodium chloride (NaCl), instead of 6-OHDA. For initial *in vivo* analyses, electrode cables were routed to the outside as previously described [14] and STELLA was placed in a backpack to allow for continuous monitoring STELLAs' functionality.

To analyze the fully encapsulated device, STELLA was implanted subcutaneously, placed between hip, costal arch and spin contralateral to the stimulation side. Therefore, the initial skull incision was enlarged by 2–3 cm and a pocket was formed by gently separating skin and muscle fascia using a blunt scissor. No blood vessels needed to be damaged here due to the loose connective tissue of rats. Wires were leaded medio-lateral between spine and ears to avoid skin irritation, otherwise the rat may scratch open the wound [35]. In 4 of 5 rats, the stimulator was fixed subcutaneously at the target pocket using the eyelet through a small (∼0.5 mm) abdominal extra incision. At the end of the implantation procedure, the full (BIST) functionality of the STELLA device was executed. After the procedure, all incisions were completely closed with simple interrupted stitches. The whole surgical procedures including animal care during the surgery are described in detail in the supplementary implantation manual.

2.5.3. Animal cohorts

Four differently treated groups of animals are reported in this study.

Group A: Naive rats with an implanted STELLA device, DBS-on ($n = 5$).

Group B: Naive rats with STELLA carried in a backpack, DBS-on ($n = 5$).

Group C: Rats with a 6-OHDA Hemi–Parkinson induction, carrying STELLA in a backpack, DBS-on ($n = 17$).

Group D: Rats with a 6-OHDA Hemi-Parkinson sham induction, carrying STELLA in a backpack, DBS-off ($n = 4$).

The groups are contributed as follows to the results: figures 7(a), (d) and (e) (A, B), figures 7(b) and (c) (A, B, C), figures 7(f) (A) and figures 8(a)–(d) (A, D).

2.5.4. Stimulation

Rats were continuously stimulated unilaterally using setting (1) in table 2 (100 μA, 60 μs, 130 Hz) from day 0 (fully implanted animals) or day 7/8 (backpack animals) after implantation until the end of the experiment (see figure 7(a)). Stimulation was paused on day 28 for behavioral testing and 24 h before the end of experiment followed by a 4 h stimulation period to provide sufficient time for c-Fos expression [48–50]. The functionality of STELLA was tested daily non-invasive using the magnetic BIST function.

2.5.5. Oscilloscope measurements

Backpack rats were regularly narcotized (isoflurane inhalations narcosis, 5% initial dose for 1 min, 2% steady-state dose) so that STELLA's stimulation output could be monitored by an oscilloscope as described in section 2.4. Same measurements were performed for rats carrying a STELLA implant on day 42 after implantation under deep anesthesia (combination of ketamine (100 mg kg^{-1} BW) and xylazine (5 mg kg^{-1} BW) intraperitoneal, 2% isoflurane), directly before sacrifices. To expose subcutaneous wires, a small abdominal incision (~5 mm) was set on the skin (after shaving).

2.5.6. Behavioral testing

Rats (groups A, B) were assessed for body weight, stress score (weight change [0–20 point], general condition [0–20 points] and spontaneous behavior [0–20 point]; 0 = no stress, 1–5 = mild stress, 6–15 = moderate stress, >15 = severe stress; higher scores indicate higher stress, maximal score = 60) and wound healing using an adapted version of the human wound score by Lippert [51] on a daily basis until the end of experiment (figures 7(d)–(f)). Video documentation of animal behavior was performed daily. On day 29 after implantation, animal motor behavior was assessed in DBS-off condition (to avoid interference of effects by the implanted stimulator and potential actions of STN stimulation) using the light-dark box test (box size 50 × 50 cm, bright zone 34 × 50 cm) over a time period of 15 min [52, 53]. Video analysis was performed using EthoVision XT 8.5 software (Noldus, Wageningen, Netherlands). It is noted that we used the light-dark box test for standardized motor assessment (number of transitions between compartments and duration time in light compartment [52, 53]).

2.5.7. Immunohistochemistry and cell counting

At the end of the experiment, brain tissue was fixated by transcardial perfusion (for 40 min with 4% paraformaldehyde), electrodes were removed, and the entire brains were kept in 4% paraformaldehyde for 24 h, transferred to 30% sterile sucrose until dehydration after 2–3 days and stored at −80 °C.

For double immunostaining, coronal brain slices (30 μm) were obtained and stained as described previously [10, 54] with the following primary antibodies: chicken anti-NeuN (1:1000; Millipore Cat# ABN91, RRID:AB_11205760) and rabbit anti-c-Fos (1:1000; Cell Signaling Technology Cat# 2250, RRID:AB_2247211). Respective secondary antibodies were as follows: Cy3-conjugated donkey anti-chicken IgG (1:500; Jackson ImmunoResearch Labs Cat# 703-165-155, RRID:AB_2340363), Alexa Fluor 488-conjugated donkey anti-rabbit IgG (1:500, Invitrogen, Molecular Probes Cat# A-21206, RRID:AB_2535792). To preserve immunofluorescence, slices were mounted with Prolong Antifade Diamond (Thermo Fisher Scientific) and stored at 4 °C until microscopy. Images were taken confocal-like with Axio.Observer.Z1 with Apotome using ZEN blue 2.3 software with Tiles and Position module (all from Carl Zeiss, Oberkochen, Germany). Every sixth slice with electrode tip artefact was imaged at 20× magnification (and five optical sections with the Apotome). Total number of c-Fos^{-}/NeuN^{+} neurons and c-Fos^{+}/NeuN^{+} neurons were counted within an area of 200 μm surrounding of the electrode tip. For adequate presentation, cell numbers were calculated to cells per mm^3.

2.5.8. Statistics

Group differences were analyzed with Mann–Whitney-*U* test for nonparametric distribution of values and with Kaplan–Meier statistics for error-free device survival (SPSS, Version 25.0, IBM, US). $p < 0.05$ was considered statistically significant with a confidence interval of 95%.

3. Results

3.1. Battery runtime, size and weight

STELLA's low current consumption for different configurations allows for an excellent adaption of the battery regarding weight, size, and stimulation time for the specific animal experiments without seriously affecting the animal's well-being. Figure 1 compares

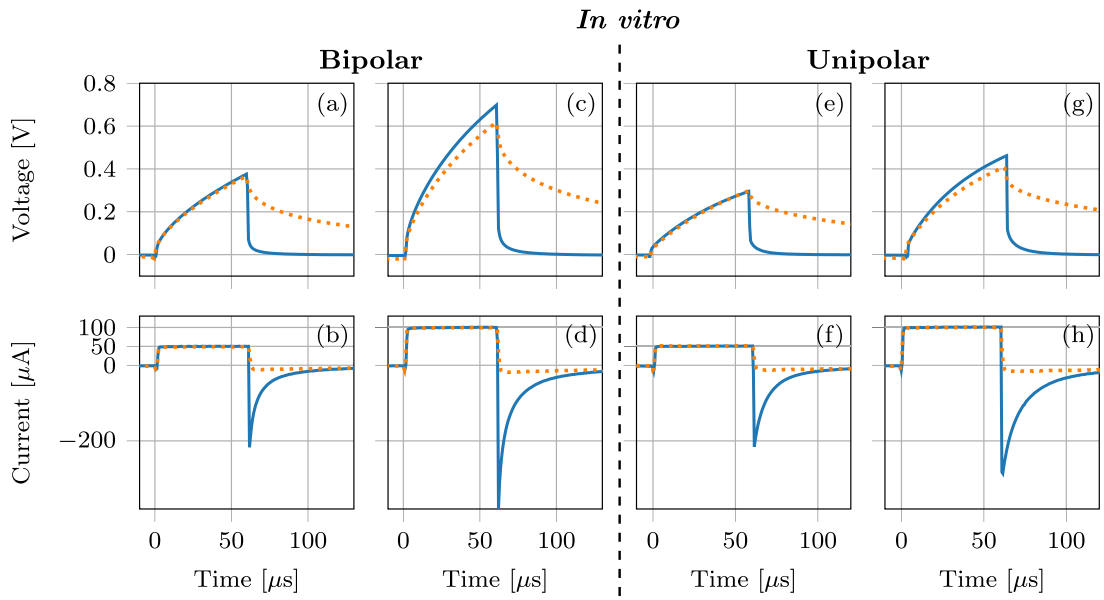

Figure 5. Representative voltage and current recordings of STELLA with a bipolar (a)–(d) and unipolar (e)–(h) electrode configuration immersed *in vitro* in 0.9% saline solution. All readings were recorded with a stimulation setting of 60 μs and 130 Hz with different current amplitudes: 50 μA (a), (b) and (e), (f), 100 μA (c), (d) and (g), (h). The blue waveforms represent recordings without a discharge resistance in the shortening path showing reversal pulses, whereas the orange dashed waveforms represent recordings with the flattening effect of adequate discharge resistances of 23.6 kΩ $\pm$ 8% for (a), (b) and (c), (d) and 19.7 kΩ $\pm$ 8% for (e), (f) and (g), (h).

stimulation time and volume (both with and without battery, not including encapsulation) of previously published neurostimulators with STELLA. It shows that STELLA achieves excellent stimulation time in a very small footprint. Together with biocompatible epoxy resin encapsulation, this enables long-term neurostimulation experiments for freely moving small laboratory animal models such as rats, mice and hamsters. The physical parameters of the fully implantable STELLA device with CR1225 battery used in our preclinical testing in rats are as follows: size: Ø17.0 $\times$ 9 mm (dimensions), 2.04 ml (volume), 4.00 $\pm$ 0.04 g (weight of device including battery, electrodes and encapsulation). The backpack system equipped with the STELLA device had a total weight of 10.75 $\pm$ 0.24 g ($n = 5$). The results are summarized in table 1 and figure 1. The physical dimensions widely used in other preclinical chronic instrumentations in small laboratory animals such as osmotic minipumps are in the reference range of 0.05–0.08 ml g^{-1} body weight (volume) and/or 0.04–0.13 g g^{-1} body weight (weight; www.alzet.com, www.opensourceinstruments.com). STELLA is thus suitable for animal sizes of approx. >20 g for STELLA with CR1216 battery (adult mice of several strains) or approx. >30 g body weight for STELLA/CR1225 (young to adult rats and adult hamsters of all strains). Together, we developed fully-implantable battery-driven STELLA stimulation systems in a small size and a weight below ~10% of the specific rodent's weight including sufficient shelf life of several months and a safety clearance of at least 2 weeks stimulation time for most preclinical DBS study designs.

3.2. Leakage testing and functionality of STELLA

Initially, we tested the long-term stability of the ready-to-use STELLA implant (as shown in figure 4) in leakage tests as described in the section 2. No sign of erosive changes or malfunction were observed during 12 weeks.

Furthermore, *in vitro* testing for two different electrode types was conducted to confirm correct functionality of the stimulator. For this, we injected stimulation pulses from STELLA through bipolar (PI-SNEX-100) and unipolar electrodes in 0.9% saline solution as shown in figure 5. The results show accurate and charge-balanced constant current pulses regarding amplitude, pulse-form, and pulse-width. The voltage waveforms result from current level and load impedance with varying electrode-configuration. The current pulses demonstrate a high reversal pulse without a discharge resistance in the shortening path (blue solid lines) whose level depends on the amount of injected charge and electrode configuration. However, an appropriate resistance adjusted by the digital potentiometer allows to flatten these reversal pulses, thus extending the discharge time (orange dashed lines). Figures 5(c) and (g) (orange dashed lines) illustrate even the case if the discharge period increases to the point where the accumulated charge is not fully discharged in between the stimulation pulses indicated by a voltage drift downwards. This drift is caused by the blocking capacitor which removes the DC offset while guaranteeing that no DC current flows. Furthermore, this setup allowed us to evaluate the BIST by generating faulty patterns like shortened electrodes or open circuits.

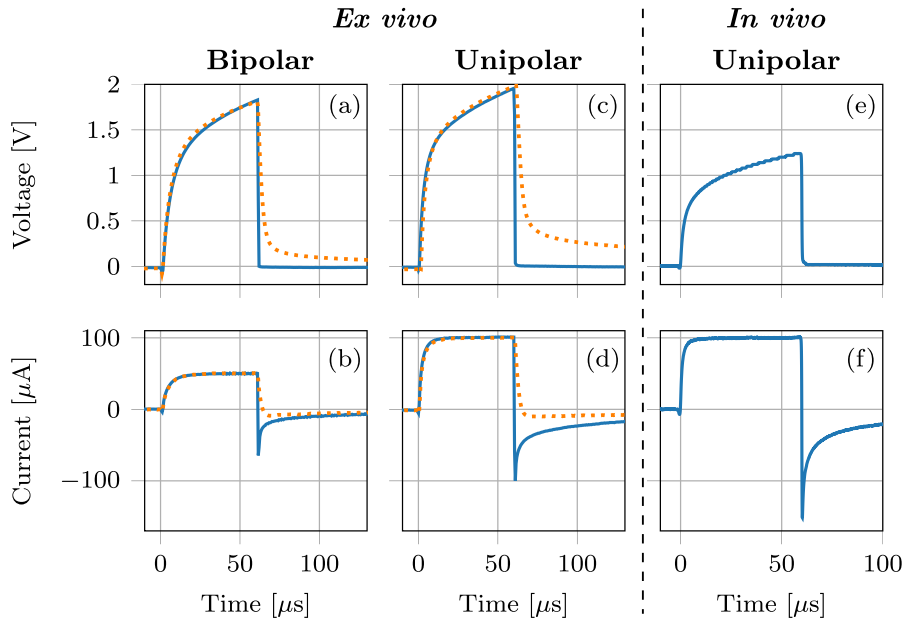

Figure 6. The picture presents voltage and current recordings of STELLA with bipolar and unipolar electrode configurations immersed *ex vivo* in brain tissue (a)–(d) and *in vivo* 42 d after STELLA implantation (e), (f). The stimulation parameters were chosen with respect to table 2. The blue waveforms represent the recordings without a discharge resistance in the shortening path showing reversal current pulses. Instead, the orange dashed waveforms represent the recordings with adequate discharge resistances of 19.6 kΩ ± 8% for (a), (b) and 39.2 kΩ ± 8% for (c), (d) achieving the damping effect of the reversal current pulses.

Although testing in saline solution is suitable for general functionality checks, they do not reflect impedance levels under real conditions in brain tissue due to their high conductive nature. To address this aspect, we immersed bipolar (PI-SNEX-100) and unipolar electrodes *ex vivo* into brain tissue by injecting stimulation pulses from STELLA as shown in supplementary figure S2(a). As in saline solution, the results in brain tissue show accurate and charge-balanced constant current pulses regarding amplitude and pulse-width (figure 6). Only the pulse-form differs slightly regarding a moderately higher but tolerable rising time. In contrast, the voltage recordings (see figures 6(a) and (c)) depict that a significantly higher stimulation voltage is required to maintain the current pulses.

3.3. Preclinical testing of long-term DBS using STELLA

First *in vivo* studies with an external predecessor of the STELLA architecture was conducted by the authors demonstrating the efficacy of short-term DBS of the entopeduncular nucleus (EPN, homologous to the globus pallidus interna in primates) over 3 h in the dt^{sz} hamster as a model of dystonia [15].

To demonstrate long-term functional stability and reliability *in vivo*, STELLA was initially carried in a backpack by young adult rats (∼12 weeks of age; $n = 5$ naive rats, $n = 17$ 6-OHDA rats; unipolar electrodes, unilateral STN stimulation) to allow regular oscilloscope measurements. Results of reliability indicated by BIST function (figure 7(b), $n = 22$), maximum stimulation voltage at the end of the pulse (100 μA, 130 Hz, 60 μs) (figure 7(c), n = 22), as well as biological tolerance (figures 7(d)–(f), $n = 5$) were compared with results from implanted STELLA devices ($n = 5$).

As shown in figure 7(b), we observed error-free function of all fully implanted STELLA devices over the whole stimulation period of 42 days, while backpack devices showed a median error-free functioning time of only 9 days. However, all devices showed stimulation voltage amplitudes below the maximum compliance voltage ensuring stable current-driven pulses (100 μA, 130 Hz, 60 μs) on day 7/8 in backpack and on day 42 in fully implanted animals (figure 7(c)). As in our *in vitro* and *ex vivo* brain studies, the results in backpack and fully implanted STELLA devices *in vivo* showed accurate and charge-balanced constant current pulses regarding amplitude and pulse-width and shape over time (see figures 6(e) and (f)).

Assessments of animal welfare and behavior over the whole stimulation period clearly revealed normal weight gain of fully implanted animals and almost no stress from 7th postoperative day until the end of observation (figures 7(d) and (e)). Indeed, regular video documentation (supplementary video) demonstrated healthy social behavior and well-being of the animals. A light-dark box test showed doubled activity of rats with an implant compared to rats with

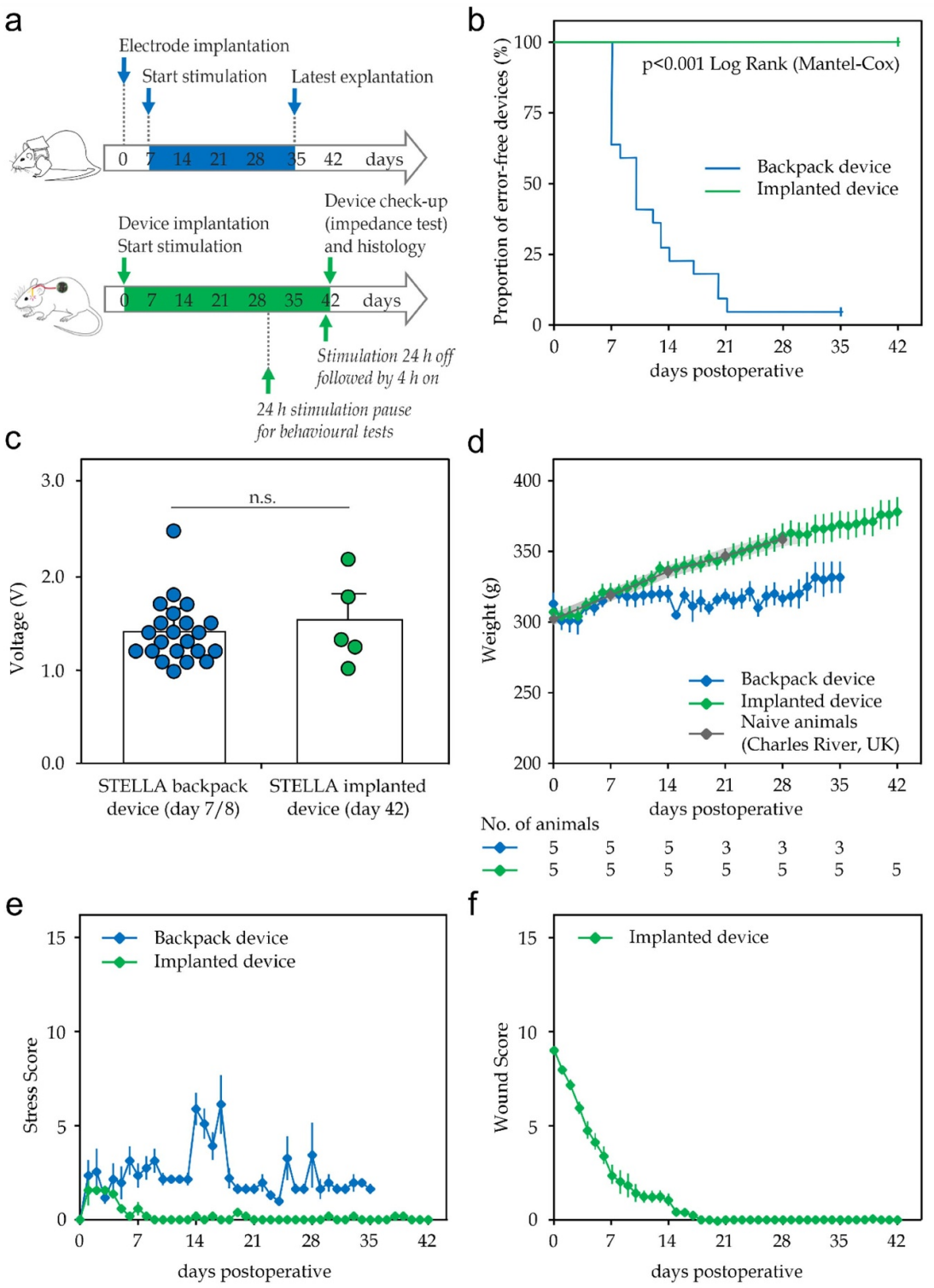

Figure 7. (a) Schematic representation of experimental paradigm for preclinical characterization of the STELLA neurostimulation device. STELLA was tested in a backpack model (blue scheme) and fully implanted model (green scheme). Schematic depictions of rat model adapted from Badstübner *et al* [14] and from https://webstockreview.net/clipart-mouse-experimental/2964091.html. (b) Kaplan–Meier plot of error-free device survival for backpack devices ($n = 22$) and fully implanted STELLA devices ($n = 5$). (c) Maximum voltage at the very end of the pulse (100 μA, 130 Hz, 60 μs) on day 7/8 in backpack ($n = 22$) and on day 42 in fully implanted animals ($n = 5$). N.s., not significant (Mann–Whitney U test). (d) Time course of body weight of rats at the time-points after electrode implantation (day 0 = day of surgery) until sacrifice (weights of stimulation devices were not compensated [backpack device: 5.79 ± 0.10 g (device and cables) plus 5.45 ± 0.03 g for backpack applied on day 7 ($n = 5$); fully implanted device including cables: 4.57 ± 0.04 g; $n = 5$]). For easy comparison, the weight course of non-instrumented male Wistar-Han rats is depicted in grey (±s.e.m. range in bright grey; data from www.criver.com). Numbers below diagram display the number of animals still under investigation on a weekly basis. (e) Time course of stress score (0 = no stress, 1–5 = mild stress; 6–15 = moderate stress, >15 = severe stress; higher scores indicate higher stress, maximal score = 60) in animals as in (d). (f) Time course of wound healing as determined using the wound score (0 = healed wound; higher scores indicate less healed wound conditions, maximal score = 26) in animals as in (d). For details on scores, refer to the section 2. Data are mean ± s.e.m.

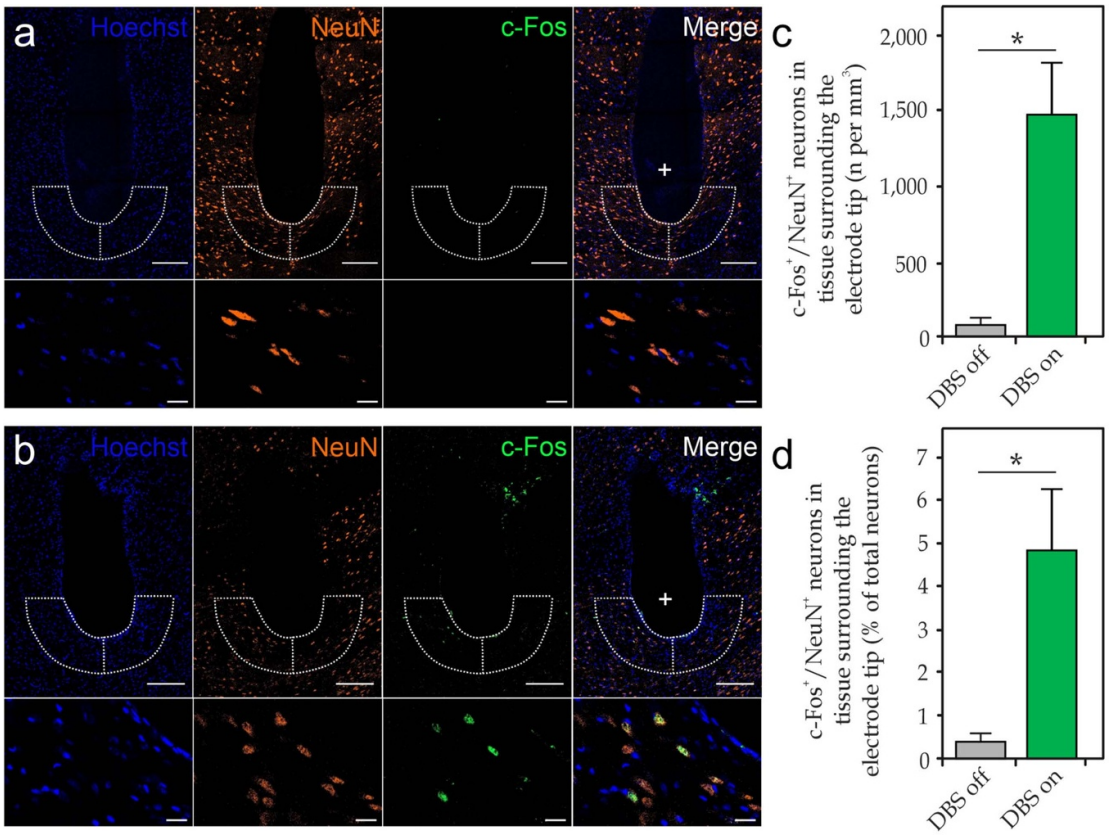

Figure 8. (a), (b) Representative fluorescence images of tissue surrounding the electrode tip in DBS-off (a) and DBS-on (b) condition. For DBS-on condition, STELLA devices were turned off for 24 h followed by a stimulation period of 4 h directly before tissue harvesting. Sections were then stained against NeuN as a marker for neurons and c-Fos to explore DBS-dependent cell activation. Non-stimulated animals with electrode placement were used as controls. Cell nuclei were counterstained with Hoechst (blue). The artifact by the electrode is marked by '+'. Detail views (lower rows) show co-expression of NeuN and c-Fos. Scale bars, 200 μm (upper rows), 20 μm (lower rows). (c), (d) Quantitative immunohistochemistry in an area of 200 μm surrounding the electrode tip (marked by dashed line in (a) and (b)) revealed significantly increased absolute numbers of c-Fos$^+$/NeuN$^+$ neurons as well as increased proportion of c-Fos$^+$ neurons normalized to total neuron population around the electrode tip in DBS-on as compared to DBS-off condition. Total number of NeuN$^+$ neurons showed no significant difference between the animal groups with 16 499 $\pm$ 625 neurons mm^{-3} in DBS-off versus 39 945 $\pm$ 10 576 neurons mm^{-3} in DBS-on animals; $p = 0.114$ (Mann–Whitney U-test; $n = 4$). * represents $p < 0.05$ (Mann–Whitney U-test; $n = 4$).

a backpack (supplementary figure S3(a)), while no differences in anxiety were observed (supplementary figure S3(b)). This is in large contrast to backpack animals with no weight gain and temporary and unpredictable increased stress by the backpack device itself, which might interfere with behavioral outcome studies (figure 7(e), supplementary figure S3(a)). Daily assessment of wound healing demonstrated fast wound healing without complications in all implanted animals after 1–2 weeks (figure 7(f)).

As a biological read-out of successful STN stimulation, the expression of the immediate early gene c-Fos was tested after a 4 h stimulation period (with 24 h DBS-off mode before) at the end of the implantation period of 42 d (DBS-on: n = 4 naive rats (group A), DBS-off: $n = 4$ sham 6-OHDA rats (group D), with STN electrode placement, but without stimulation). As shown in figure 8, stimulation of the rat STN for 4 h with stimulation parameters set at 100 μA, 130 Hz and a pulse width of 60 μs, provoked a higher expression of c-Fos in STN neurons surrounding the electrode as compared to non-stimulated control STN neurons. These data demonstrate biological functionality of the STELLA neurostimulation device after long-term use of 42 days.

4. Discussion

We present STELLA, a preclinical neurostimulator implant tackling the unmet necessity for reproducible, ultra-long DBS studies in small rodents. STELLA combines a high level of miniaturization with an ultra-low power consumption for a DBS setup in small laboratory animals such as rodents. Our calculations predict an unprecedented battery runtime for continuous stimulation in DBS-rodent experiments of up to 3 years using a CR2032 battery. All results including software, hardware schematics and documentation are published freely available for peer production, usage, reproduction or modification. The experimental *in vivo* studies reveal that the chosen range of compliance voltage is valid and that a unified voltage design is possible for most

applications, yielding less components with nearly no power penalty. In combination with a careful selection of components and optimized choice of operating points, we achieved tremendous power savings.

Our results demonstrate that a modular discrete version of STELLA exceeds the requirements for most DBS small animal studies by far and realizes runtimes more than tenfold of the previous state of research with less volume (see figure 1). This enables completely new animal studies of long-term stimulation effects. If short-term experiments are desired, even tiny 1.5 V batteries are possible, which further minimize volume and weight. Modularity, affordable pricing at low quantities and easy adaptability towards the needs of other researchers are important requirements for the practical use of the preclinical stimulator. Therefore, we prefer a discrete PCB solution over technologies that offer a higher level of integration like application-specific integrated circuits.

A unified modeling approach of battery, electronics, and stimulation using SystemC-AMS [55] helped to define an ultra-low power extensible architecture which minimizes active and leakage currents and incorporates salient features for animal experiments like failure-monitoring, software-controlled stimulation parameters and charge balancing. An SPI-based extension bus supports further stackable modules like radio and readers essential for closed-loop approaches. Finally, a custom medical grade epoxy resin-based encapsulation methodology protects the stimulator and battery in a lightweight package within a tiny footprint tailored for implantation in small laboratory animals.

Furthermore, the feasibility of programming stimulation parameters (amplitude, frequency and pulse width) allows a broad scope of experimental implantation. In future studies, the different effects of long-term DBS-on the several disease models, such as PD or dystonia, can be investigated with the same stimulation system. As shown in [15], the value of stimulation frequency is essential for the therapeutic success in dystonic hamsters. Note that once STELLA is fully encapsulated and implanted, reflashing the firmware is no longer possible. However, the stimulation setting is not always known prior to implantation and may need to be adjusted at a later timepoint. For this purpose, the Hall sensor can be used to sequentially step through pre-programmed stimulation settings by manually applying a magnetic field. After each change of the stimulation setting, BIST serves to verify whether the stimulation with new parameters is valid. This enables preclinical research into a wide range of scientific questions to identify optimal stimulation parameters.

Most available solutions for DBS devices for small animals are either cable-bound, need (large) head mountings, restrict free movement or influence behavioral testing such as through the need of special cages (see table 1 for details [21, 22, 24–29, 31, 34, 56]). Only very few devices provide the opportunity to fully implant the whole system but show some limitations concerning energy consumption, reliable and reproducible operation, stimulation patterns, long-term *in vivo* characterization after implantation and/or specifications are not completely available as open source data to the scientific community [30, 32, 33, 57]. We exemplarily applied the proposed fully implanted STELLA device for DBS of the subthalamic nucleus to adult rats over a period of 6 weeks and compare these data with the previously reported technology using backpacks [14].

Rats with backpacks are not only restricted in movement, but also in their cleaning behavior, getting stuck with their teeth or claws during scratching or grooming in the backpack. Caught teeth in backpacks lead to massive loss of saliva and following weight, until they got freed. Additionally, they are not able to regularly eat during this time. Thus, they require very frequent and intensive monitoring intervals. Moreover, if the backpack is not sufficiently tight, the rats may take it off and thereby lose their stimulator. In order to free animals, repair broken wires or reattach backpacks and stimulator, it is most often necessary to narcotize them. This is stressful for the animals, impacts behavioral studies and consumes experimental time. Simultaneously, such failures interrupt the stimulation for an unknown period subsequently reducing experimental control and validity. Those events are detectable as peaks in daily measurements of weight curve and stress score (figures 7(d) and (e)) or appear as errors as shown in figure 7(b). Rats with implants do not show any of these problems. They are completely free in movement, grooming, scratching, exploring, sleeping and social behavior. They show no signs of wound infection or irritation after implantation in contrast to backpacked rats, which have an open wound because of wires routed to the outside.

Although the small number of animals in our cohorts limits the reliability of statistical analysis, our data demonstrate that fully-implanted STELLA neurostimulators were very well-tolerated over 42 days without relevant stress after the early postoperative phase resulting in unrestricted animal behavior. Encapsulation, external control and monitoring of function proved to be feasible. Moreover, stimulation showed accurate and charge-balanced constant current pulses regarding amplitude, pulse-width, frequency and shape in all measurements we performed over the whole experimental time period. Stimulating effects on brain tissue on the biological levels were proven with the increase of c-Fos expression in neurons of the DBS target area [48–50, 57].

Together, by introducing STELLA as a reliable DBS device for rodent models of neurological disorders under a fully open source license, we help to address major issues according to the 3R principle

of humane experimental techniques [59, 60]. Indeed, STELLA will not only dramatically reduce animal stress (refinement) but also help to minimize animal numbers (reduction) by its high reliability of long-term DBS and thus reducing drop-outs during the stimulation period.

5. Conclusion

We propose STELLA as a low-cost dual-channel fully implantable, scalable and reliable neurostimulator for small laboratory animals. With this DBS device, we address the urgent need for reverse translational research on DBS in freely moving rodent disease models with the important opportunity of performing sensitive behavioral experiments including e.g. Water Maze testing. STELLA thus also addresses important issues of animal research by refinement of experimental paradigms and technology and reduction of animal numbers according to the 3R principle of humane experimental techniques. All hardware, software and additional materials are available under an open source license.

Data availability

All data that support the findings of this study are included within the article (and any supplementary files). Data for PCB, firmware and additional materials are available under an open-source license at https://github.com/SFB-ELAINE/STELLA/

Acknowledgments

This research was supported by the Deutsche Forschungsgemeinschaft (DFG, German Research Foundation) through the Collaborative Research Centre CRC 1270 'Electrically Active Implants' (DFG; SFB 1270/1–299150580) to A R, R K, D T and A S M F was supported by the CRC 1270 'Electrically Active Implants' (DFG; SFB 1270/1–299150580) through the rotation position program for clinician scientists. Many researchers in ELAINE helped in starting this project. The special support by Kathrin Badstübner-Meeske, Uta Naumann, Valentin Neubert, Uwe Knüpfer, Julius Zimmermann, Peter Kumm, Cornelius Knuth, Thomas Kröger-Badge and Franz Markert is greatly appreciated [58].

Conflicts of interest

The authors declare no conflict of interest.

ORCID iDs

Franz Plocksties https://orcid.org/0000-0003-0433-7703
Maria Kober https://orcid.org/0000-0003-1034-1960
Christoph Niemann https://orcid.org/0000-0001-9371-1087
Dirk Timmermann https://orcid.org/0000-0001-9267-9695

References

[1] Krack P, Martinez-Fernandez R, Del Alamo M and Obeso J A 2017 Current applications and limitations of surgical treatments for movement disorders *Mov. Disord.* **32** 36–52
[2] Mably A J and Colgin L L 2018 Gamma oscillations in cognitive disorders *Curr. Opin. Neurobiol.* **52** 182–7
[3] Raza C, Anjum R and Shakeel N U A 2019 Parkinson's disease: mechanisms, translational models and management strategies *Life Sci.* **226** 77–90
[4] Aldehri M, Temel Y, Alnaami I, Jahanshahi A and Hescham S 2018 Deep brain stimulation for Alzheimer's disease: an update *Surg. Neurol. Int.* **9** 58
[5] Wathen C A, Frizon L A, Maiti T K, Baker K B and Machado A G 2018 Deep brain stimulation of the cerebellum for poststroke motor rehabilitation: from laboratory to clinical trial *Neurosurg. Focus* **45** E13
[6] Hamani C and Nobrega J N 2010 Deep brain stimulation in clinical trials and animal models of depression *Eur. J. Neurosci.* **32** 1109–17
[7] Jakobs M, Fomenko A, Lozano A M and Kiening K L 2019 Cellular, molecular, and clinical mechanisms of action of deep brain stimulation-a systematic review on established indications and outlook on future developments *EMBO Mol. Med.* **11** 4
[8] Paschen S and Deuschl G 2018 Patient evaluation and selection for movement disorders surgery: the changing spectrum of indications *Prog. Neurol. Surg.* **33** 80–93
[9] Baunez C and Gubellini P 2010 Effects of GPi and STN inactivation on physiological, motor, cognitive and motivational processes in animal models of Parkinson's disease *Prog. Brain Res.* **183** 235–58
[10] Fauser M, Ricken M, Markert F, Weis N, Schmitt O, Gimsa J, Winter C, Badstübner-Meeske K and Storch A 2021 Subthalamic nucleus deep brain stimulation induces sustained neurorestoration in the mesolimbic dopaminergic system in a Parkinson's disease model [in eng] *Neurobiol. Dis.* **156** 105404
[11] So R Q, McConnell G C and Grill W M 2017 Frequency-dependent, transient effects of subthalamic nucleus deep brain stimulation on methamphetamine-induced circling and neuronal activity in the hemiparkinsonian rat [in eng] *Behav. Brain Res.* **320** 119–27
[12] McConnell G C, So R Q and Grill W M 2016 Failure to suppress low-frequency neuronal oscillatory activity underlies the reduced effectiveness of random patterns of deep brain stimulation [in eng] *J. Neurophysiol.* **115** 2791–802
[13] Reese R, Charron G, Nadjar A, Aubert I, Thiolat M-L, Hamann M, Richter A, Bezard E and Meissner W G 2009 High frequency stimulation of the entopeduncular nucleus sets the cortico-basal ganglia network to a new functional state in the dystonic hamster *Neurobiol. Dis.* **35** 399–405
[14] Badstuebner K *et al* 2017 Deep brain stimulation of hemiparkinsonian rats with unipolar and bipolar electrodes for up to 6 weeks: behavioral testing of freely moving animals *Parkinsons Dis.* **2017** 5693589
[15] Paap M *et al* 2021 Deep brain stimulation by optimized stimulators in a phenotypic model of dystonia: effects of different frequencies *Neurobiol. Dis.* **147** 105163
[16] Musacchio T, Rebenstorff M, Fluri F, Brotchie J M, Volkmann J, Koprich J B and Ip C W 2017 Subthalamic nucleus deep brain stimulation is neuroprotective in the

A53T alpha-synuclein Parkinson's disease rat model *Ann. Neurol.* **81** 825–36
[17] Fischer D L *et al* 2017 Subthalamic nucleus deep brain stimulation does not modify the functional deficits or axonopathy induced by nigrostriatal alpha-synuclein overexpression *Sci. Rep.* **7** 16356
[18] Fischer D L, Kemp C J, Cole-Strauss A, Polinski N K, Paumier K L, Lipton J W, Steece-Collier K, Collier T J, Buhlinger D J and Sortwell C E 2017 Subthalamic nucleus deep brain stimulation employs trkB signaling for neuroprotection and functional restoration *J. Neurosci.* **37** 6786–96
[19] Fischer D L, Collier T J, Cole-Strauss A, Wohlgenant S L, Lipton J W, Steece-Collier K, Manfredsson F P, Kemp C J and Sortwell C E 2015 High-frequency stimulation of the rat entopeduncular nucleus does not provide functional or morphological neuroprotection from 6-hydroxydopamine *PLoS One* **10** e0133957
[20] Nowak K *et al* 2011 Optimizing a rodent model of Parkinson's disease for exploring the effects and mechanisms of deep brain stimulation *Parkinsons Dis.* **2011** 414682
[21] Adams S D, Bennet K E, Tye S J, Berk M and Kouzani A Z 2019 Development of a miniature device for emerging deep brain stimulation paradigms *PLoS One* **14** e0212554
[22] Arfin S K, Long M A, Fee M S and Sarpeshkar R 2009 Wireless neural stimulation in freely behaving small animals *J. Neurophysiol.* **102** 598–605
[23] Ewing S G, Porr B, Riddell J, Winter C and Grace A A 2013 SaBer DBS: a fully programmable, rechargeable, bilateral, charge-balanced preclinical microstimulator for long-term neural stimulation *J. Neurosci. Methods* **213** 228–35
[24] Fluri F, Mutzel T, Schuhmann M K, Krstić M, Endres H and Volkmann J 2017 Development of a head-mounted wireless microstimulator for deep brain stimulation in rats *J. Neurosci. Methods* **291** 249–56
[25] Forni C, Mainard O, Melon C, Goguenheim D, Kerkerian-Le Goff L and Salin P 2012 Portable microstimulator for chronic deep brain stimulation in freely moving rats *J. Neurosci. Methods* **209** 50–57
[26] Kolbl F, N'Kaoua G, Naudet F, Berthier F, Faggiani E, Renaud S, Benazzouz A and Lewis N 2016 An embedded deep brain stimulator for biphasic chronic experiments in freely moving rodents *IEEE Trans. Biomed. Circuits Syst.* **10** 72–84
[27] Kouzani A Z, Kale R P, Zarate-Garza P P, Berk M, Walder K and Tye S J 2017 Validation of a portable low-power deep brain stimulation device through anxiolytic effects in a laboratory rat model *IEEE Trans. Neural Syst. Rehabil. Eng.* **25** 1365–74
[28] Liu H, Wang C, Zhang F and Jia H 2017 An implantable device for neuropsychiatric rehabilitation by chronic deep brain stimulation in freely moving rats *Neuroreport* **28** 128–33
[29] Pinnell R C, Pereira De Vasconcelos A, Cassel J C and Hofmann U G 2018 A miniaturized, programmable deep-brain stimulator for group-housing and water maze use *Front. Neurosci.* **12** 231
[30] Alpaugh M, Saint-Pierre M, Dubois M, Aubé B, Arsenault D, Kriz J, Cicchetti A and Cicchetti F 2019 A novel wireless brain stimulation device for long-term use in freely moving mice *Sci. Rep.* **9** 6444
[31] De Haas R, Struikmans R, Van Der Plasse G, Van Kerkhof L, Brakkee J H, Kas M J H and Westenberg H G M 2012 Wireless implantable micro-stimulation device for high frequency bilateral deep brain stimulation in freely moving mice *J. Neurosci. Methods* **209** 113–9
[32] Harnack D, Meissner W, Paulat R, Hilgenfeld H, Müller W-D, Winter C, Morgenstern R and Kupsch A 2008 Continuous high-frequency stimulation in freely moving rats: development of an implantable microstimulation system *J. Neurosci. Methods* **167** 278–91
[33] Hentall I D 2013 A long-lasting wireless stimulator for small mammals *Front. Neuroeng.* **6** 8
[34] Millard R E and Shepherd R K 2007 A fully implantable stimulator for use in small laboratory animals *J. Neurosci. Methods* **166** 168–77
[35] Chang P, Hashemi K S and Walker M C 2011 A novel telemetry system for recording EEG in small animals *J. Neurosci. Methods* **201** 106–15
[36] Gimsa U, Schreiber U, Habel B, Flehr J, Van Rienen U and Gimsa J 2006 Matching geometry and stimulation parameters of electrodes for deep brain stimulation experiments–numerical considerations *J. Neurosci. Methods* **150** 212–27
[37] Gimsa J, Habel B, Schreiber U, Rienen U V, Strauss U and Gimsa U 2005 Choosing electrodes for deep brain stimulation experiments–electrochemical considerations *J. Neurosci. Methods* **142** 251–65
[38] Salatino J W, Ludwig K A, Kozai T D and Purcell E K 2017 Glial responses to implanted electrodes in the brain *Nat. Biomed. Eng.* **1** 862–77
[39] Piallat B, Chabardes S, Devergnas A, Torres N, Allain M, Barrat E and Benabid A L 2009 Monophasic but not biphasic pulses induce brain tissue damage during monopolar high-frequency deep brain stimulation *Neurosurgery* **64** 156–62 (discussion 162–153)
[40] Scheiner A, Mortimer J T and Roessmann U 1990 Imbalanced biphasic electrical stimulation: muscle tissue damage *Ann. Biomed. Eng.* **18** 407–25
[41] Merrill D R, Bikson M and Jefferys J G R 2005 Electrical stimulation of excitable tissue: design of efficacious and safe protocols *J. Neurosci. Methods* **141** 171–98
[42] Sooksood K, Stieglitz T and Ortmanns M 2009 An experimental study on passive charge balancing *Adv. Radio Sci.* **7** 197–200
[43] Patrick E, Orazem M E, Sanchez J C and Nishida T 2011 Corrosion of tungsten microelectrodes used in neural recording applications *J. Neurosci. Methods* **198** 158–71
[44] Kirschstein T *et al* 2020 Stereotactically injected Kv1.2 and CASPR2 antisera cause differential effects on CA1 synaptic and cellular excitability, but both enhance the vulnerability to pro-epileptic conditions *Front. Synaptic Neurosci.* **12** 13
[45] Würdemann T *et al* 2016 Stereotactic injection of cerebrospinal fluid from anti-NMDA receptor encephalitis into rat dentate gyrus impairs NMDA receptor function [in eng] *Brain Res.* **1633** 10–18
[46] Klatte K, Kirschstein T, Otte D, Pothmann L, Muller L, Tokay T, Kober M, Uebachs M, Zimmer A and Beck H 2013 Impaired D-serine-mediated cotransmission mediates cognitive dysfunction in epilepsy [in eng] *J. Neurosci.* **33** 13066–80
[47] Paxinos G and Watson C 2007 *The Rat Brain in Stereotaxic Coordinates* (New York: Academic)
[48] Herrera D G and Robertson H A 1996 Activation of c-fos in the brain *Prog. Neurobiol.* **50** 83–107
[49] Schulte T, Brecht S, Herdegen T, Illert M, Mehdorn H M and Hamel W 2006 Induction of immediate early gene expression by high-frequency stimulation of the subthalamic nucleus in rats *Neuroscience* **138** 1377–85
[50] Pfluger P, Pinnell R C, Martini N and Hofmann U G 2019 Chronically implanted microelectrodes cause c-fos expression along their trajectory *Front. Neurosci.* **13** 1367
[51] Lippert H 2006 *Wundatlas (Wound Atlas)* (Stuttgart: Georg Thieme Verlag) (https://doi.org/10.1055/b-002-35728)
[52] Arrant A E, Schramm-Sapyta N L and Kuhn C M 2013 Use of the light/dark test for anxiety in adult and adolescent male rats *Behav. Brain Res.* **256** 119–27
[53] Serchov T, Van Calker D and Biber K 2016 Light/dark transition test to assess anxiety-like behavior in mice *Bio-Protocol* **6** 4

[54] Markert F, Muller L, Badstubner-Meeske K and Storch A 2020 Early chronic intermittent maternal hyperoxygenation impairs cortical development by inhibition of Pax6-positive apical progenitor cell proliferation *J. Neuropathol. Exp. Neurol.* **79** 1223–32
[55] Heller J *et al* 2020 Towards virtual prototyping of electrically active implants using systemC-AMS *Methods and Description Languages for Modelling and Verification of Circuits and Systems GMM/ITG/GI Workshop 2020*
[56] Ewing S G, Lipski W J, Grace A A and Winter C 2013 An inexpensive, charge-balanced rodent deep brain stimulation device: a step-by-step guide to its procurement and construction *J. Neurosci. Methods* **219** 324–30
[57] Fleischer M, Endres H, Sendtner M and Volkmann J 2020 Development of a fully implantable stimulator for deep brain stimulation in mice *Front. Neurosci.* **14** 726
[58] Plocksties F GitHub Repository 2021 The SofTware dEfined impLantabLe modular plAtform (STELLA) for preclinical deep brain stimulation (https://github.com/SFB-ELAINE/STELLA/)
[59] Russell W M S and Burch R L 1959 *The Principles of Humane Experimental Technique* (Baltimore, MD: Johns Hopkins Center for Alternatives to Animal Testing (CAAT))
[60] Richmond J 2002 Refinement, reduction, and replacement of animal use for regulatory testing: future improvements and implementation within the regulatory framework *ILAR J.* **43** S63–68